

This item is the archived peer-reviewed author-version of:

On/off resonance Raman optical activity of human serum transferrin

Reference:

Bogaerts Jonathan, Johannessen Christian.- On/off resonance Raman optical activity of human serum transferrin
Journal of Raman spectroscopy - ISSN 0377-0486 - 50:5(2019), p. 641-646
Full text (Publisher's DOI): <https://doi.org/10.1002/JRS.5570>
To cite this reference: <https://hdl.handle.net/10067/1581900151162165141>

on/off resonance Raman optical activity of human serum transferrin

Jonathan Bogaerts^a, Christian Johannessen^{a,*}

^a Molecular Spectroscopy Group, Department of Chemistry, University of Antwerp, Belgium

Abstract

The transferrin proteins exhibit two high affinity Fe(III) binding pockets and are responsible for the iron transport into cells of higher order organisms. Previously, transferrins have been studied as possible transporter molecules for drugs delivery. In this study, Raman optical activity (ROA) was employed to investigate human serum transferrin. Due to the presence of Fe(III) in the holo form of the protein, it is in resonance with the the laser excitation wavelength (of 532 nm) used in the experiments. Consequently resonance enhanced ROA bands were observed in the spectrum of the holo form. Nevertheless, far from resonance bands, arising from the protein backbone, could simultaneously be observed in the ROA spectrum of the holo form. This implies that ROA can be used to provide simultaneously information on the metal binding pocket as well as on the secondary structure of the protein. Furthermore, it was found that the amount of observed resonance enhanced ROA signals can be tuned by partially removing the iron present in the protein. Electronic circular dichroism (ECD) was employed to verify the Raman/ROA results.

Keywords: Raman optical activity, Raman spectroscopy, Transferrin, Resonance enhancement

Introduction

Since its inception in the early 70's, Raman optical activity (ROA) has been widely employed to determine the absolute configuration^{1,2}, and to study the solution phase structure of (bio)molecules, including carbohydrates and proteins.³ In general, ROA relies on the small difference in intensity of Raman scattered right- and left circularly polarised light from chiral molecules. In far from resonance (FFR) conditions, ROA has been proven to be very sensitive to the secondary structure of proteins in aqueous solution and to subtle structural changes within a secondary structure element.⁴⁻¹⁰ However, ROA is intrinsically a weak phenomena ($\sim 10^{-4}$ smaller than the corresponding Raman signal). Therefore, methods that are able to increase the ROA signal are much sought after. One of the strategies that has successfully been explored in recent years, is the use of resonance enhancement. In resonance ROA (RROA), coupling of specific vibrational modes to the allowed electronic transitions of the absorbing chromophore results in a selective enhancement of these vibrational modes. Therefore, RROA of proteins containing a chromophore, which is in resonance with the used laser excitation wavelength, can provide structural information of that chromophore in the protein, such as the planarity of the porphyrin ring in haemproteins.^{11,12}

Here we report a (R)ROA study on human serum transferrin (HuTf). Transferrins (Tf) are glycoproteins with molecular mass around 80 kDa and play an important role in the iron transportation and metabolism, which is necessary for cell growth, of higher order organisms.¹⁴ The N-terminus and C-terminus of the protein fold up independently to give two major structural

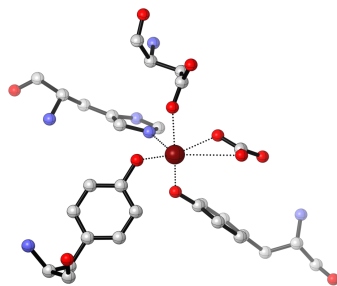


Figure 1: Fe^{3+} binding pocket of the N-lobe of human serum transferrin (PDB id. 1N84).¹³ The hydrogen atoms are omitted for clarity. The figure was made using CYLview v1.0 BETA.

domains. Each domain bears a specific, high-affinity Fe(III) binding site. The Fe^{3+} ion is bound very tightly in an octahedral coordination (shown in Fig.1) involving two tyrosinates, one histidine, one aspartic acid and is mediated by one bidentate which, under physiological conditions, is a carbonate.^{15,16} The most striking feature of this property is that the binding is reversible with decreasing pH.¹⁷⁻¹⁹ Therefore Tf can appear in different forms: The holo-form of Tf is fully saturated with bound iron. The iron-depleted form is referred to as apotransferrin (apoTf). Studies by Aisen *et al.*²⁰ and Williams *et al.*²¹ showed that structural differences between the domains result in unequal binding of metals to the two sites. Therefore, Tf can also appear in a monoferric form termed siderotransferrin (sideroTf).

The transporter role of Tf has caught the attention of medicinal chemists to produce a wide range of Tf based pharmaceutical applications. The (bio)pharmaceutical role of Tf is to bind to other therapeutics with short half-lives and improve the pharmacokinetics of these drugs by extending their activity.^{22,23} Previous Raman spectroscopy studies by Ashton *et al.*²⁴ focussed on the determination of the glycosylated status and iron binding of transferrin in off resonance conditions. In this study, we extend this work, to the best of the author's knowledge, for the first time to a combined on/off RROA study of HuTf. We show that the resonance properties of Tf can be tuned by changing the amount of Fe^{3+} bound to the protein, which makes (R)ROA a very suitable technique for analysing HuTf in its holo-, sidero-, and apo form.

Materials and methods

Samples and sample preparation

holoTf and sideroTf, both from human serum, were obtained from Sigma-Aldrich (Saint Louis, MO, USA) and Lee biosolution (Maryland Heights, MO, USA), respectively, as lyophilized powders. All other chemicals were procured from Carl Roth GmbH (Karlsruhe, Germany). ApoTf was prepared from holoTf by addition of 500 μL of a 0.2 M Na_2EDTA solution to 20 mg of holoTf in 10 mL 0.1 M acetate buffer (pH 5). After 24 hours the solution was dialysed against Tris.HCl buffer (pH 8).

The lyophilised powders were dissolved in deionised water to a concentration of 50 mg mL^{-1} . The apoTf was concentrated to a similar concentration using a 10 kDa cut-off spin filter (Viva-spinTM, GE Healthcare). The final solutions were loaded into a micro - fluorescence quartz cell (Starna Scientific Ltd., 4x4x3 mm internal dimensions) and used for Raman and ROA measurements.

For electronic circular dichroism (ECD) measurements in the 280 - 650 nm region, the lyophilised powders were dissolved in deionised water to a concentration of 20 mg mL^{-1} . The apoTf was diluted from the $\sim 50 \text{ mg mL}^{-1}$ to a similar concentration. The ECD measurements

in the 180 - 280 nm region, were performed on a protein concentration of $\sim 0.25 \text{ mg mL}^{-1}$. Subsequently, the samples were loaded in a SUPRASIL[®] quartz sample cell with a pathlength of 0.5 mm and used for ECD measurements.

Raman and ROA measurements

Raman and ROA spectra were measured simultaneously using the previously described Chiral-RAMAN-2X scattered circular polarization (SCP) ROA instrument (BioTools, Inc.)^{6,25,26} running at a resolution of 7 cm^{-1} . The Raman intensities are displayed as the sum ($I_R + I_L$) and the ROA intensities as the difference ($I_R - I_L$) in circular intensities with I_R and I_L denoting for the inelastic Raman scattering with right and left circular polarization, respectively. The laser excitation wavelength was 532 nm. The laser power was set at the source in the range of 500-800 mW depending on the sample, and total acquisition times were between 22 and 48 hours at ambient temperature. Solvent spectra were subtracted from the Raman spectra after which the baseline correction procedure by Boelens *et al.*²⁷ was applied. Cosmic ray spikes were removed from the ROA data by means of a median filter. To correct the distorted baseline in the ROA spectra, a third-order, 401-points Savitzky-Golay filter was applied on the raw ROA spectra. This creates a featureless baseline, which was then subtracted from the raw ROA spectra. Subsequently, the baseline corrected ROA spectra were smoothed using a third-order, nine-points Savitzky-Golay filter. These different treatments together with the plotting of the spectra were applied in MATLAB software version R2016b (The MathWorks, Natwick, MA, USA).

ECD measurements

The ECD measurements were carried out on a Chirascan[™]-Plus instrument (Applied Photo-physics Ltd.) and are reported in units of ellipticity. The experiments were performed at $20 \text{ }^\circ\text{C}$, with a scan speed of 120 nm min^{-1} , scan step of 1 nm and bandwidth of 1 nm. The spectra were collected under constant nitrogen flow and scans were performed from 280 to 180 nm (the secondary structure range) and from 650 to 280 nm (the aromatic/chromophore range). The ECD spectra were baseline corrected by subtracting the solvent background, measured at the same conditions. The plotting of the spectra were applied in MATLAB software version R2016b (The MathWorks, Natwick, MA, USA).

Results and Discussion

The laser employed in this study is in resonance with the ligand-to-metal-charge transfer (LMCT) band found in holoTf²⁸ (see top right spectrum of Fig. 2). As a result, the Raman spectrum of the holoTf (top left spectrum in Fig.3) reveals four resonance enhanced bands at 1170 cm^{-1} , 1284 cm^{-1} , 1506 cm^{-1} and 1608 cm^{-1} , which can be assigned to phenolate vibrational modes.²⁹ Remarkably, the Fe-O vibrations, found at $\sim 425 \text{ cm}^{-1}$ ²⁴, is not enhanced by the resonance effect. The corresponding ROA (top right spectrum in Fig.3) bands are all positive and opposite in sign to the electronic circular dichroism of the resonant electronic transition (see top right Fig.2) as predicted by the single electronic state (SES) theory.³⁰ The same theory predicts that the circular intensity difference (CID) value, defined as $\frac{I_R - I_L}{I_R + I_L}$, is minus one half of the ECD anisotropy ratio g_{ECD} . The CID values for the resonance enhanced bands are summarised in Table S1 (Supporting Information) together with the value of $-1/2 g_{\text{ECD}}$ at 532 nm. Although the sign and the order of magnitude of the CID values are in line with $-1/2 g_{\text{ECD}}$, the exact value of the CID is highly dependent on the baseline corrections performed on both the Raman and ROA spectra. These baseline corrections were necessary due to strong intrinsic fluorescence from the samples. As a result, the CID values deviate from the value predicted by the SES theory. In

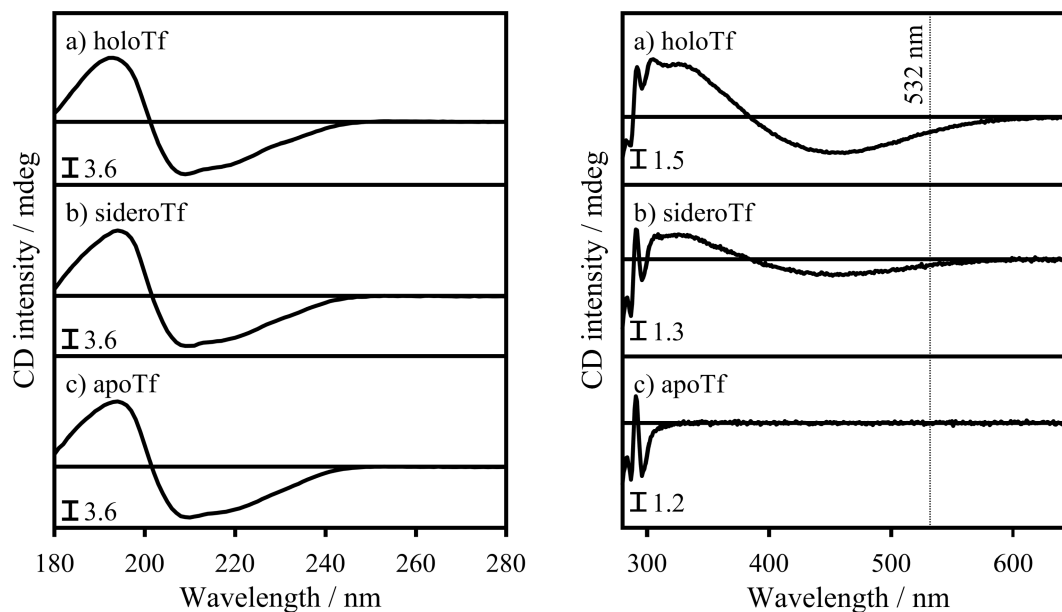


Figure 2: Left: ECD spectra of $\sim 0.25 \text{ mg mL}^{-1}$ aqueous solutions of a) holoTf, b) sideroTf and c) apoTf in the secondary structure region. The spectra are normalised according to the absorbance at 190 nm of holoTf. Right: ECD spectra of $\sim 20 \text{ mg mL}^{-1}$ aqueous solutions of a) holoTf, b) sideroTf and c) apoTf in the 280 - 650 nm region. The spectra are normalised according to the absorbance at 280 nm. The absorbance spectra are shown in Fig.S1 (Supporting Information). A close-up of the 400 - 600 nm range of the absorption spectra are shown in Fig.S2 (Supporting Information).

addition to the resonance enhanced bands, a $-/+$ couplet in the amide I region, centered around 1662 cm^{-1} and arising from the carbonyl stretch vibration, is observed, which indicates a β -sheet conformation of the protein.^{4,5} Furthermore, a negative band is observed at $\sim 1450 \text{ cm}^{-1}$. As these vibrations arise from the protein backbone itself, and not from the chromophore, these do not have to adhere to the SES theory. This means that both phenomena of RROA and FFRROA are observed at the same time. Haraguchi *et al.*³¹ observed the same phenomena for a photoactive yellow protein, albeit less pronounced than in the current presented work.

When the iron is removed, the protein is no longer in resonance with the 532 nm laser. This is verified by the ECD spectrum of the apoprotein (bottom right panel in Fig.2), which does not show any signal near 532 nm. Consequently, FFR Raman and ROA spectra were recorded and are shown as the bottom spectra in Fig.3. The off resonance conditions can clearly be observed from the Raman spectrum of apoTf, which is no longer dominated by tyrosine vibrations. The ROA spectrum of apoTf, again shows a $-/+$ couplet in the amide I region centered around 1662 cm^{-1} . The amide III region, shows a prominent positive contribution at $\sim 1320 \text{ cm}^{-1}$ and is typically assigned to polyproline II (PPII) helix.³ The negative contribution at lower wavenumbers ($\sim 1249 \text{ cm}^{-1}$), may originate from the β -strands of apoTf, as assigned in the case of insulin.⁴ However care must be exerted as negative contributions in this region of the spectrum can be assigned to several different secondary structure elements. As last, a $-/+$ couplet in the backbone skeletal region, centered at $\sim 1100 \text{ cm}^{-1}$, is indicative for an α -helical contribution. Overall, the ROA spectrum suggests that the solution structure of apoTf exhibits α -helix and β -sheet combined with a large degree of unordered structure, which is line with the crystal structure of the protein.²² However, we must note that the crystal structure is taken of the iron-bound form and that it is known that the iron depleted form exerts a large conformational movement upon iron removal. Therefore, holoTf may exhibit a larger degree of order than the apo form. Nevertheless, the ECD spectra of both forms in the secondary structure region (e.g. 180 - 260 nm, shown in left Fig.2) are very similar, which means that the contribution of different

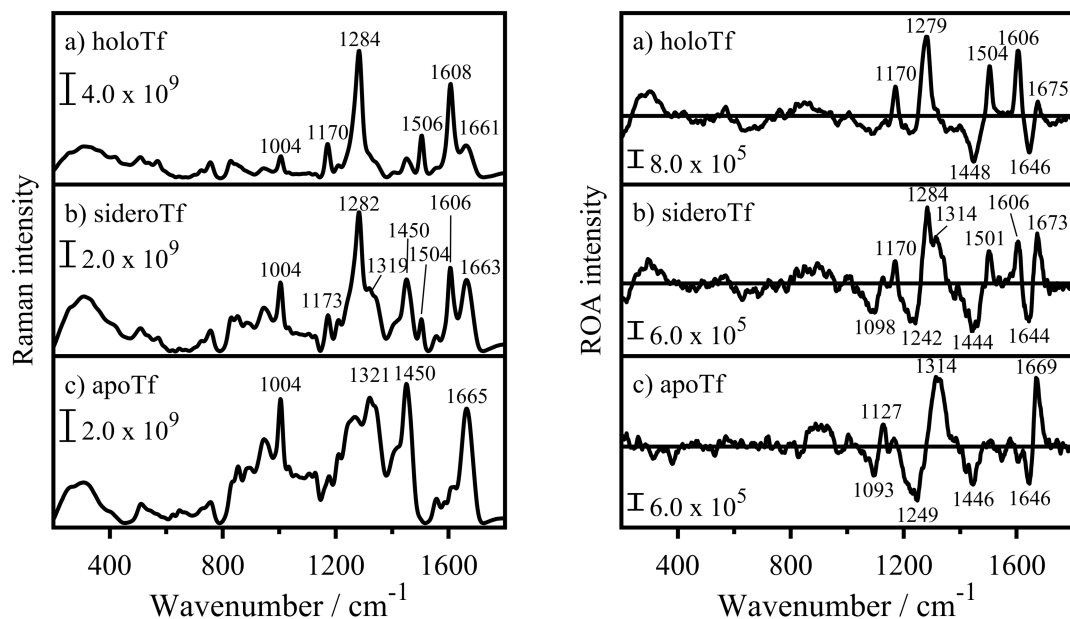


Figure 3: Raman (left) and ROA (right) spectra of $\sim 50 \text{ mg mL}^{-1}$ aqueous solutions of a) holoTf, b) sideroTf and c) apoTf.

secondary structure elements to the overall secondary structure, does not change significantly upon iron removal.

As last sideroTf is discussed. The ECD spectrum in the secondary structure region of sideroTf, shown in the middle left spectrum in Fig. 2 is again very similar as the spectra of the two other forms, which is in line with the assumption that the overall secondary structure is maintained upon iron removal. Furthermore, the spectral pattern below 300 nm (see in middle right panel of Fig.2), is remarkably similar to the pattern observed in apoTf and the spectral pattern above 300 nm show significant comparison with holoTf, although the relative intensities changes. The corresponding Raman and ROA spectra of sideroTf are represented in the middle spectra in Fig.3. The Raman spectrum shows that the ratio between resonance enhanced bands and FFR bands decreases. This change in ratio is clearly observed between the bands at 1608 cm^{-1} and 1661 cm^{-1} . Another example is found in ratio of to the resonance enhanced bands at $\sim 1170 \text{ cm}^{-1}$ and the phenylalanine band, observed at 1004 cm^{-1} . Hence, the Raman spectrum of sideroTf is composed of both resonance enhanced and normal Raman bands in an almost 1-to-1 ratio, which is a different observation than for the holoTf case. This is confirmed by the corresponding ROA spectrum (middle right spectrum in Fig.3). Indeed; the $-/+$ couplet in the backbone skeletal stretch region appears here as a $-/+$ pattern where the last positive contributions was also found in the holoTf spectrum. Furthermore, the amide III regions is conserved from the apoTf with an extra positive contribution at $\sim 1284 \text{ cm}^{-1}$, assigned to tyrosinate vibrations of the iron binding pocket (*vide supra*). Finally, the couplet in the amide I region is accompanied with a double positive contribution at the lower wavenumber side, again as seen in the holoTf ROA spectrum. Hence, measuring sideroTf using a 532 nm laser leads to Raman and ROA spectra containing both signatures of holoTf and apoTf in an almost equal amount. This means that the resonance enhancement of HuTf can be tuned by the amount of iron present in the sample.

These observations open the door to using ROA to simultaneously study the chromophore binding pocket (on resonance) and the secondary structure (off resonance) of bio-active compounds carrying metal co-factors.

Conclusion

In this study we have presented an on/off resonance Raman/ROA study of human serum transferrin. Our results have shown that the Raman spectrum of holoTf consist mainly of bands arising from resonance enhanced tyrosinate vibrations. The corresponding RROA spectrum shows both positive and negative contributions. Because some of these bands arise from the protein backbone and not from the chromophore, this observed spectral pattern is not in contradiction to the SES limit theory, which predicts a monosignate RROA spectrum. The simultaneous detection of on and off resonance ROA signals arising from a protein has only scarcely reported before. Furthermore, ROA confirms that apoTf adopts a secondary structure which is combined from α -helix, β -sheet and disordered structure in solution. The ECD spectra in the secondary structure region, for the holo-, apo- and sidero form showed that the overall secondary structure is maintained upon iron removal. The sideroTf Raman/ROA spectra are composed out of both resonance enhanced and off resonance bands, whereby simultaneously information of the chromophore and the backbone conformation of the protein can be extracted. This paves the way to use ROA to study bio-active compounds containing a metal, which is in resonance with the used laser excitation wavelength, without losing information on the protein secondary structure which is normally the case in resonance ROA.

Acknowledgement

J.B. acknowledges the Research Foundation Flanders (FWO) for the appointment of a pre-doctoral scholarship (1198318N) and the University of Ghent (IOF Advanced TT) for the purchase of the ChiralRAMAN-2X spectrometer.

References

- [1] J. Haesler, I. Schindelholz, E. Riguet, C. G. Bochet, W. Hug. *Nature* **2007**; *446*, 526.
- [2] V. Profant, A. Jegorov, P. Bouř, V. Baumruk. *J. Phys. Chem. B* **2017**; *121*, 1544.
- [3] L. D. Barron. *Biomed. Spectrosc. Imaging* **2015**; *4*, 223.
- [4] L. D. Barron, L. Hecht, E. W. Blanch, a. F. Bell. *Prog. Biophys. Mol. Biol.* **2000**; *73*, 1.
- [5] I. H. McColl, E. W. Blanch, A. C. Gill, A. G. O. Rhie, M. a. Ritchie, L. Hecht, K. Nielsen, L. D. Barron. *J. Am. Chem. Soc.* **2003**; *125*, 10019.
- [6] L. D. Barron, F. Zhu, L. Hecht, G. E. Tranter, N. W. Isaacs. *J. Mol. Struct.* **2007**; *834-836*, 7.
- [7] S. Yamamoto, M. Straka, H. Watarai, P. Bouř. *Phys. Chem. Chem. Phys.* **2010**; *12*, 11021.
- [8] C. Mensch, L. D. Barron, C. Johannessen. *Phys. Chem. Chem. Phys.* **2016**; *18*, 31757.
- [9] E. Van De Vondel, C. Mensch, C. Johannessen. *J. Phys. Chem. B* **2016**; *120*, 886.
- [10] C. Mensch, A. Konijnenberg, R. Van Elzen, A.-M. Lambeir, F. Sobott, C. Johannessen. *J. Raman Spectrosc.* **2017**; *48*, 910.
- [11] S. Abdali, C. Johannessen, J. Nygaard, T. Nørbygaard. *J. Phys. Condens. Matter* **2007**; *19*, 285205.
- [12] C. Johannessen, P. C. White, S. Abdali. *J. Phys. Chem. A* **2007**; *111*, 7771.

- [13] T. E. Adams, A. B. Mason, Q. Y. He, P. J. Halbrooks, S. K. Briggs, V. C. Smith, R. T. MacGillivray, S. J. Everse. *J. Biol. Chem.* **2003**; *278*, 6027.
- [14] R. R. Crichton, M. Charloteaux-wauters. *Eur. J. Biochem* **1987**; *164*, 485.
- [15] H. Kurokawa, B. Mikami, M. Hirose. *J. Mol. Biol.* **1995**; *254*, 196.
- [16] D. H. Hamilton, I. Turcot, A. Stintzi, K. N. Raymond. *J. Biol. Inorg. Chem.* **2004**; *9*, 936.
- [17] J. P. G. Miller, D. J. Perkins. *Eur. J. Biochem.* **1969**; *10*, 146.
- [18] G. E. Norris, B. F. Anderson, E. N. Baker. *Acta Crystallogr. B.* **1991**; *47*, 998.
- [19] P. K. Bali, O. Zak, P. Aisen. *Biochemistry* **1991**; *30*, 324.
- [20] P. Aisen. *J. Biol. Chem.* **1978**; *253*, 1930.
- [21] J. Williams, K. Moreton. *Biochem. J.* **1980**; *185*, 483.
- [22] P. T. Gomme, K. B. McCann. *Drug Discov. Today* **2005**; *10*, 267.
- [23] I. Nakase, B. Gallis, T. Takatani-Nakase, S. Oh, E. Lacoste, N. P. Singh, D. R. Goodlett, S. Tanaka, S. Futaki, H. Lai, T. Sasaki. *Cancer Lett.* **2009**; *274*, 290.
- [24] L. Ashton, V. L. Brewster, E. Correa, R. Goodacre. *Analyst* **2017**; *142*, 808.
- [25] W. Hug, G. Hangartner. *J. Raman Spectrosc.* **1999**; *30*, 841.
- [26] W. Hug. *Appl. Spectrosc.* **2003**; *57*, 1.
- [27] H. F. Boelens, R. J. Dijkstra, P. H. Eilers, F. Fitzpatrick, J. A. Westerhuis. *J. Chromatogr. A* **2004**; *1057*, 21.
- [28] M. G. Patch, C. J. Carrano. *Inorganica Chim. Acta* **1981**; *56*, L71.
- [29] B. P. Gaber, V. Miskowski, T. G. Spiro. *J. Am. Chem. Soc.* **1974**; *96*, 6868.
- [30] L. A. Nafie. *Chem. Phys.* **1996**; *205*, 309.
- [31] S. Haraguchi, M. Hara, T. Shingae, M. Kumauchi, W. D. Hoff, M. Unno. *Angew. Chemie - Int. Ed.* **2015**; *54*, 11555.